

γ -Ray Pulsars: Emission Zones and Viewing GeometriesRoger W. Romani¹ and I.-A. Yadigaroglu

Department of Physics, Stanford University, Stanford, CA 94305-4060

ABSTRACT

There are now a half dozen young pulsars detected in high energy photons by the Compton GRO, showing a variety of emission efficiencies and pulse profiles. We present here a calculation of the pattern of high energy emission on the sky in a model which posits γ -ray production by charge depleted gaps in the outer magnetosphere. This model accounts for the radio to γ -ray pulse offsets of the known pulsars, as well as the shape of the high energy pulse profiles. We also show that $\sim 1/3$ of emitting young radio pulsars will not be detected due to beaming effects, while $\sim 2.5\times$ the number of radio-selected γ -ray pulsars will be viewed only high energies. Finally we compute the polarization angle variation and find that the previously misunderstood optical polarization sweep of the Crab pulsar arises naturally in this picture. These results strongly support an outer-magnetosphere location for the γ -ray emission.

Subject headings: pulsars — gamma rays — polarization

1. Introduction

Since the birth of γ -ray astronomy the two most prominent galactic point sources have been identified with young rotation-powered pulsars, the Crab and Vela pulsars. The site of γ -ray production has however been intensely debated for almost two decades. The two principal models are the ‘polar cap’ picture exemplified by the work of Daugherty and Harding (1982) and the ‘outer gap’ model championed by Cheng, Ho and Ruderman (1988, CHR). In the former acceleration occurs near the neutron star surface and the observed emission results from a $\gamma - B$ pair cascade. In the second model acceleration is posited in charge depleted regions near the speed of light cylinder and $\gamma - \gamma$ pair production is an important process. We have examined these two models (Chiang and Romani 1992) and find that the observed pulse profiles arise most

¹Alfred P. Sloan Fellow

naturally in a modified version of the outer gap picture. Moreover, spectral calculations (Chiang and Romani 1994, CR94) have shown that in this model emission processes vary throughout the magnetosphere and can produce spectral variations through the pulse like those seen. In this paper we quantitatively compare the outer gap predictions with the observed profiles, supporting these conclusions.

The impetus for these computations is the dramatic increase in information on the γ -ray pulsars provided by the *Compton Gamma Ray Observatory*. In addition to improved light curves and phase resolved spectra for Crab and Vela (*e.g.* Nolan *et al.* 1993), CGRO has detected at least four other pulsars in high-energy emission, including Geminga, which has not been seen in radio emission (*e.g.* Thompson, *et al.* 1992, Ulmer, *et al.* 1993, Fierro, *et al.* 1993, Mayer-Hasselwander *et al.* 1994). Other bright plane sources await confirmation as pulsars, and the expected number of each of these classes of objects is presently unknown. It is apparent from these data that older rotation-powered pulsars are increasingly efficient producers of γ emission, at least for characteristic ages $\lesssim 10^{5.5} - 10^6$ y. In deciphering the puzzle of γ production efficiencies upper limits on other pulsars are also important. Their interpretation is, however, unclear. Finally detailed information on the location of the emission region is an essential tool for understanding the polarization and spectrum seen from the observed pulsars. The geometrical computations of pulsar beaming in this paper address each of these issues.

2. Emission Zone Geometry and Profile Calculation

Well above the neutron star surface the dipole component of the magnetic field will dominate. We have computed the location of the outer magnetosphere charge depletion regions (outer gaps) by calculating the dipole field structure from the full retarded potentials. The outer gaps (CHR) are regions above the null charge surface (where the co-rotation charge density changes sign) extending to the speed of light cylinder, where co-rotation must break down. Accordingly plasma lost from this gap cannot be replenished from the stellar surface and a charge depleted region with significant $\mathbf{E} \cdot \mathbf{B}$ is developed. This is the location of the particle acceleration which gives rise to the observed γ -ray emission. Following CHR, we assume that the outer gap will be bounded below by the surface of last closed field lines. We determine this surface by finding the dipole field lines which are tangent to speed of light cylinder. Traced back to the stellar surface, these give a polar cap moderately extended in longitude for significant magnetic inclinations α . The upper gap surface will be along field lines for which substantial $\gamma - \gamma$ pair production shorts out the outer gap. It is this upper surface, where the population of accelerated pairs builds up to appreciable densities, that in fact constitutes the emission zone of the gap.

This emission surface lies significantly within the open field line region above the polar cap. We find (*c.f.* Chiang and Romani 1994) the soft photons supporting the $\gamma - \gamma$ pair production that

limits gap growth are provided principally from regions in the inner magnetosphere (the lowest portions of the gap, where synchrotron losses are significant) or from the stellar surface. Pair production will be strongest close to this soft photon source, and so we assume that the gap width for a given position around the polar cap is determined by this pair production at the null charge surface. Two effects determine the pair production length and hence the gap width at this point. First as one moves to the sides of the polar cap, the intersection of the null charge surface with the last closed line moves higher in the magnetosphere. There the soft photon flux at the threshold for pair creation on the curvature γ from primaries accelerated to radiation reaction limited energies in the gap will decrease – this tends to increase the pair production length. Countering this to some extent, the angle between the central soft flux and the locally produced high energy γ 's will increase higher in the magnetosphere – this lowers the pair creation threshold and for a steep soft spectrum from thermal or synchrotron radiation, decreases the pair production length. The complete solution of the gap growth and radiation production is a complex non-linear problem (CR94). Here we adopt a simple scaling law for the gap width w at the null charge surface which approximates these behaviors $w \propto r_c$, with r_c the local field line radius of curvature and with the width at the gap's lowest point scaling as α^{-1} . This lowest width can also depend on the P and B , thereby controlling the pulsar luminosity – this has not been treated in detail. Thus gap regions starting at high altitude will be wider. However, the gap width does not grow as fast as the $B \sim r^{-3}$ spreading of the field lines; the flux threaded towards the sides of the gap decreases. Along any given field line, charges will flow above the null charge surface, so we take the set of field lines determined above to define the gap upper surface (Figure 1).

We note that we have not included the effects of particle inertia on the field lines or the field perturbations induced by magnetospheric currents. These should be small in our near vacuum region as long as we are not very close to the light cylinder. In particular these produce only small changes in the geometry of the polar cap. Moreover, we wish to emphasize that the majority of our results are quite robust to perturbations of the field geometry and are thus independent of the details of how we have chosen our gap surface. However, fine structure in observed pulse profiles can help detail the precise location of the high energy emission zone. The brightness along the gap builds up as the particle density increases, but then falls off as the light cylinder is approached. As an estimate of this variation we take $F \propto 2s - s^2$, where s is the arc length along the field line measured in units of the light cylinder radius, and impose an exponential cutoff at $s = 1$ with $\sigma = 0.5$.

With the emission zone defined, we note the radiating particles will have significant γ factors along the field lines. High energy photons will thus be radiated in a narrow beam tangent to the emission zone. As E_γ decreases below an MeV, an increasing fraction of the emission will arise from lower energy pairs and the inverse-Compton and synchrotron photons producing the observed pulse will have a larger spread about the field line (CR94). However, significant flux will still be along the local field line and so the high energy beam shape is defined by the tangent to this last closed surface. Aberration effects and light travel delays will be very significant high in

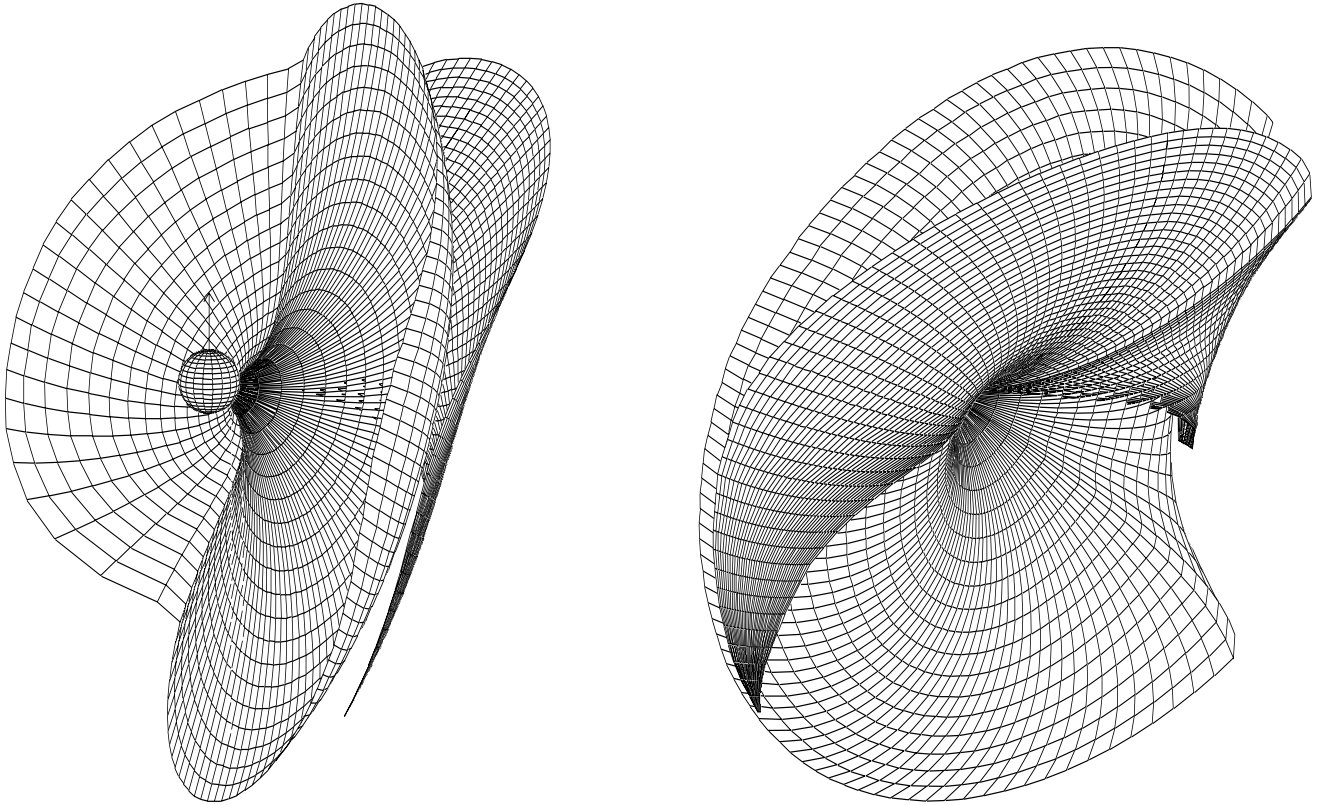


Fig. 1.— Two views of the surface of last closed field lines, cut at $1.2r_{LC}$ for an $\alpha = 70^\circ$ rotator (see text). The gap lies above the null charge surface, inside the open field line region. We show the illuminated section of the the gap upper surface. The observed pulsar γ -rays are beamed along this surface. The neutron star’s radius is increased to $0.1r_{LC}$ for clarity.

the magnetosphere, so we account for these and bin the observed radiation into pulse profiles. We display this as a skymap in pulsar phase and observer co-latitude ($\zeta = \alpha + \beta$). In Figure 2 we show the radio caps (from both hemispheres) along with the γ -ray beam from the Southern radio cap. Angles and the indicated line of sight are those appropriate to the Vela pulsar.

2.1. Gamma Ray Beam Characteristics and Radio Data

Several features of the γ -ray beams are worth mentioning. First, since radiation occurs above the null charge surface, where $\mathbf{\Omega} \cdot \mathbf{B} = 0$, γ -ray emission observed at a given ζ comes from the polar cap in the opposite hemisphere. Particles of the opposite sign from those producing the observed emission will be accelerated inward in the gap. Their radiation would be visible in the same hemisphere as the radio cap, however CR94 show that the radiation efficiency and spectrum can be quite different for the inward-going particle; we expect that they will produce little observable flux.

Second, as noted by Chiang and Romani (1992), double pulses with significant bridge emission are visible for most ζ as long as α is not too small. These pulses are caused by crossing caustic surfaces in the pulse phase sky map, where flux from a large portion of the outer gap arrives in phase. These caustics are produced only with the full effect of aberration and light travel time and can be quite sharp when the emission surface is thin. Relatively narrow γ -ray pulses will be visible for lines of sight close to the upper edge of the gamma ray beam, and will have two poorly defined peaks with strong bridge emission, such as PSR1706-44 and possibly PSR1055-52. Also very wide (width between γ -ray peaks $\Delta > 0.5$) double pulses are possible in this model, especially for small α and $\zeta \sim 90^\circ$. As α approaches 0° , regions where the outer gap approaches the light cylinder after crossing over the rotation pole become increasingly important in the pulse profile. Faint emission from this region is visible on the trailing side of the pulse in Figure 2. Near $\alpha = 0^\circ$, the γ emission is concentrated to the equator, and the region where strongly pulsed radiation is visible will be small. Those pulsars seen at small α will tend to have wide pulses.

Radio data are particularly important in constraining possible viewing geometries. In particular, polarization data can give very good determinations of β from the rotating vector model (Lyne and Manchester 1988, LM). Pulse widths can also be used to estimate α in some cases (Rankin 1990, 1993), but in general α is only poorly constrained, unless emission is visible in an interpulse or through a large range of pulsar phase. However, the radio data (especially with accurate polarization measurements) also give good measurements of the phase of the magnetic axis. The relative phase of the radio and γ pulse are now available for the observed pulsars (*c.f.* Ulmer 1994). In Figure 3 we compare the γ -ray pulse width (between peaks) as predicted from our model as a function of the phase offset from the radio with the values measured for the observed γ -ray pulsars (Table 1). The agreement is very good, although in the case of the Crab, the radio

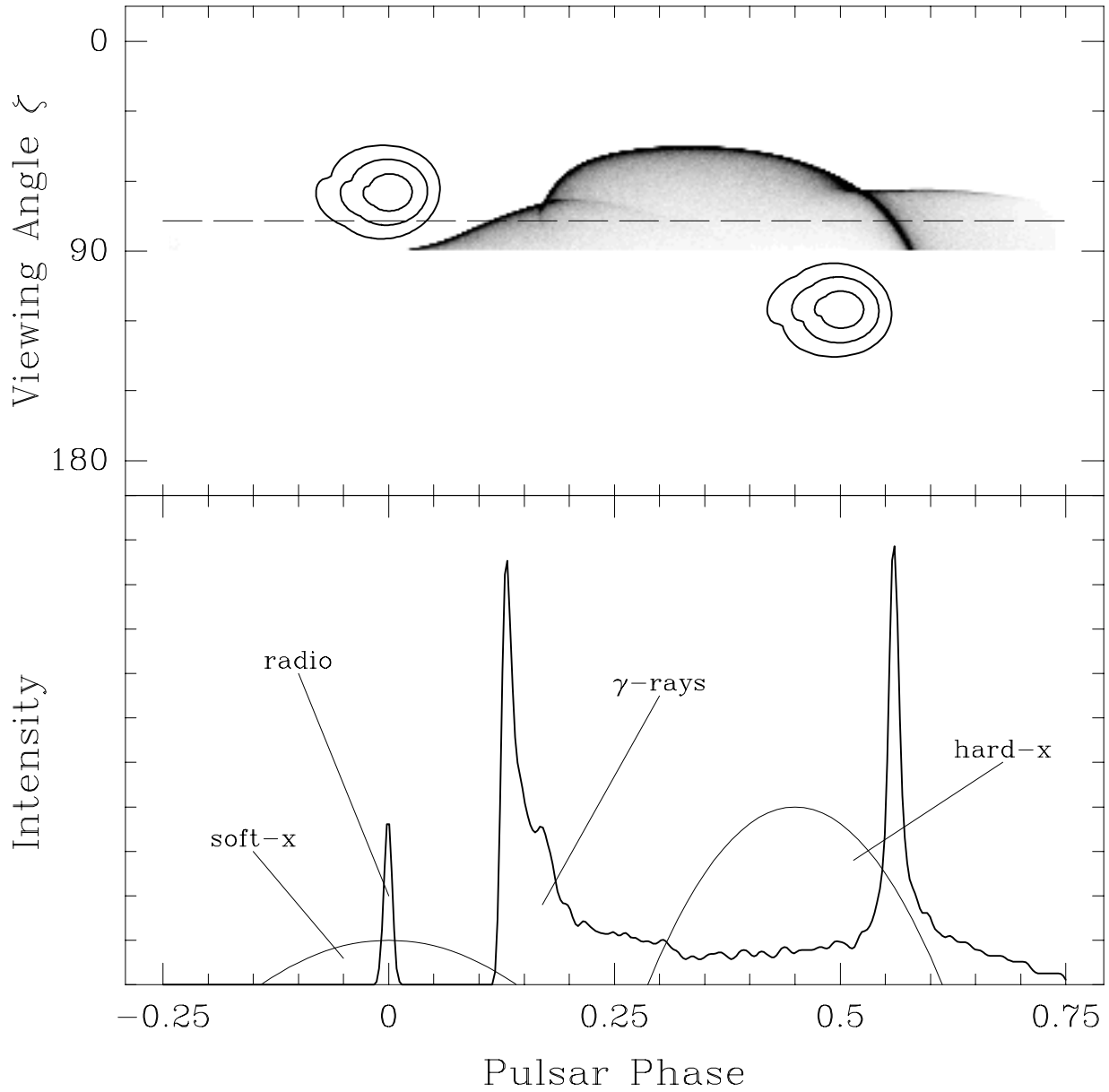


Fig. 2.— Skymap of pulsed beams and pulse profiles for Vela parameters ($\alpha = 65^\circ$). Above: Pulsar emission as a function of pulsar phase - observed lines-of-sight cut horizontally across the image at constant ζ ; the Earth line-of-sight is indicated (dashed line). Emission from the observed outer gap (half-tone) and both radio caps (contours) are shown. For clarity, the outer gap visible for $\zeta > 90^\circ$ is not shown. Below: Pulse profiles for Vela. The model γ -ray pulse for the line of sight above is indicated, along with the leading radio pulse and schematic plots of the hard (magnetospheric) and soft (thermal) X-ray pulses.

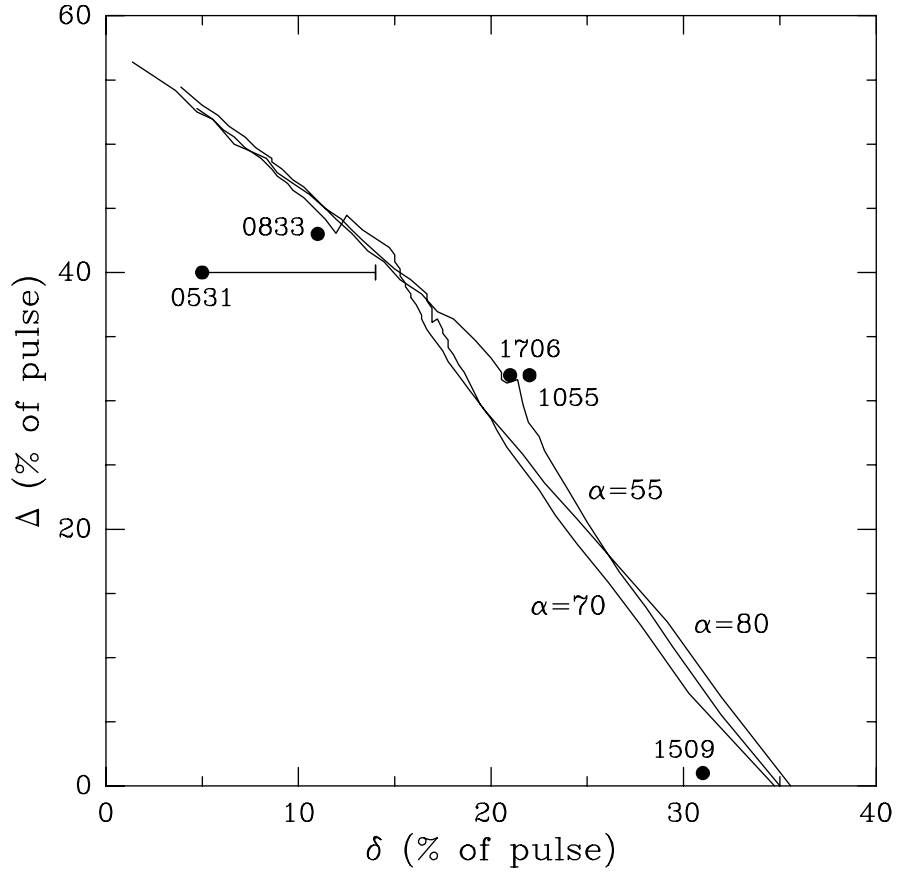


Fig. 3.— γ -ray pulse width Δ vs. lag of first γ pulse from the radio pulse δ . Observed values for radio pulsars are indicated. Model predictions for α covering the observed pulsar's range are given by the full lines. The phase of the magnetic axis for the Crab is somewhat uncertain – the horizontal bar gives 1/2 the range over which the core component is expected to appear.

emission lies slightly closer to the γ pulse than expected. However, we note that for this shortest period pulsar, the envelope in which the radio emission, identified with the precursor, can appear is relatively large. Half this range is shown by the horizontal bar. For the other pulsars more complex profiles and polarization data allow the true centroid of the radio pulse to be better determined. Overall, the good reproduction of the observed correlation is a strong success of the model.

2.2. Individual Pulsars

We have computed models for a range of α and sampled the pulse profiles of these for the full range of ζ . Figures 4a and 4b show contours of constant δ and Δ respectively in the $\alpha - \zeta$ plane. The gap width used in these sums is appropriate to a ~ 0.1 s pulsar, near the middle of the observed range. Above the line of $\Delta = 0$, no γ -ray emission is seen. Radio emission is visible for

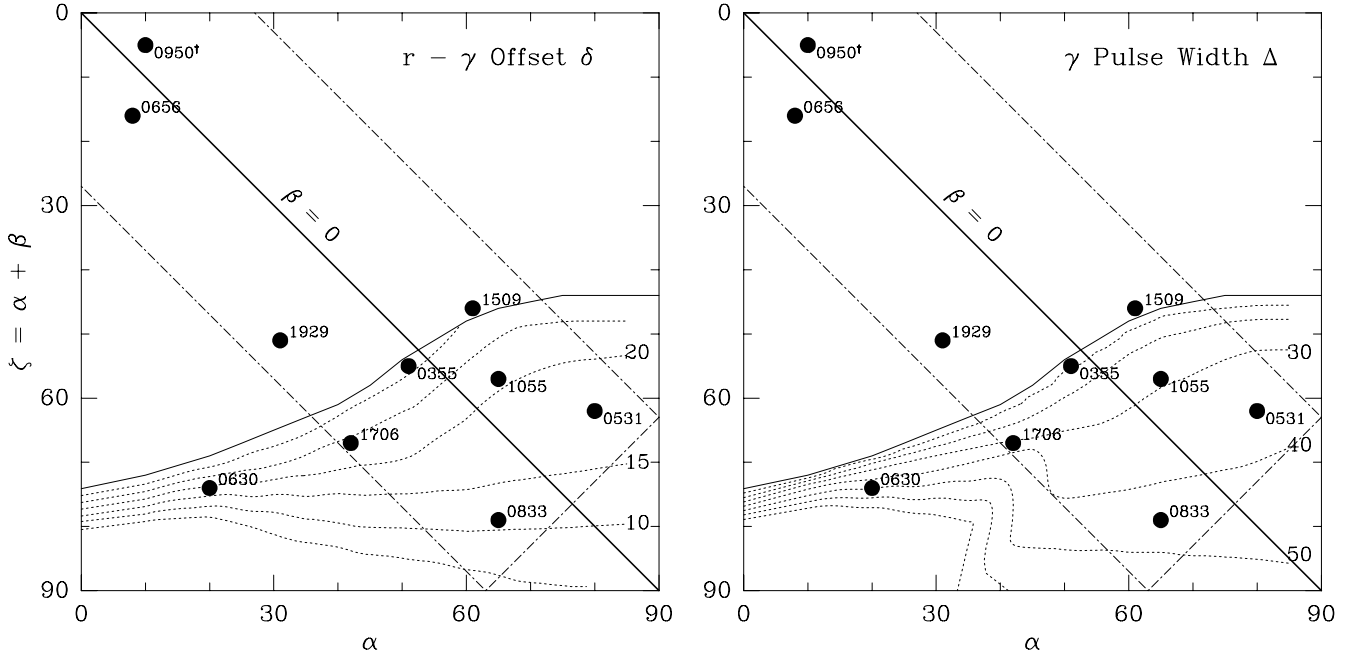


Fig. 4.— Isocontours of lag of from the radio phase δ (left) and γ -ray pulse width Δ (right) in the $\alpha - \zeta$ plane (see text). Contours are computed for a gap width appropriate to a median age ($P \sim 0.1$ s) pulsar; selected contour values are labeled near $\alpha = 90^\circ$. Observed pulsars are positioned at estimated values of (α, ζ) ; for Geminga a large range along $\Delta = 0.5$ is allowed. Pulsars known to have $\zeta > 90^\circ$ (\dagger) have been displayed reflected to the Northern hemisphere. Above the line $\Delta = 0$ no γ rays are visible; far from $\beta = 0$ pulsars will not be detected in the radio.

small β ; lines showing the range of visibility for the Crab are drawn, although at low frequencies and/or low intensities, radio flux may be visible over a wider range. Interpulsars, with α near 90° and radio emission visible from both poles are in the lower right corner of the diagram. For $\alpha > 90^\circ$ the geometry will be similar with β of opposite sign.

Using β values (and α , where available) from the radio data we have plotted positions of young pulsars on Figure 4a and 4b. In some cases, we have chosen a value of α consistent with the radio and γ -ray data. For Geminga a substantial range along $\Delta = 0.5$ is consistent with the data. Results for each of the pulsars are in good agreement with the models. Moreover several peculiarities of the observed profiles are explained with these figures. For example, it is apparent that for much of the parameter space giving $\Delta \gtrsim 0.5$, as for Geminga, β will be too large for the radio pulse to be visible. Also for nearly aligned pulsars such as PSR1929+10 (Phillips 1990), no γ pulse is expected, so the strong EGRET upper limits can not be construed to imply a luminosity cut-off at the characteristic age of PSR1929+10. Also, in several cases pulsars are located just outside the range of γ visibility (*eg.* PSR1509-58 and possibly PSR0354+55); in these cases, the GeV γ -ray beam tightly collimated to the gap surface may be missed, while the lower energy emission with its wider beam pattern may be detected. In these cases OSSE, or even X-ray energies, may provide the best hope of pulse detection.

Most importantly, this model gives significant predictions for the behavior of the radio polarization. Careful measurements should be able to check these expected viewing geometries in many cases. Conversely, polarization studies in connection with our high energy model computations can help decide when careful pulse searches of young pulsars are likely to be successful. Ultimately, knowledge of the viewing geometry will help in locating the emission region for various sectors of the pulse profile and, through phase-resolved spectra, will allow a detailed study of the emission region.

2.3. X-ray and Optical Pulses

In this paper we do not compute X-ray (0.1-10 KeV) profiles in detail. However, we note that there are several important sources of X-ray emission in this model. First we expect the region of the gap near the null charge line to be a significant source of X-ray flux for young pulsars. This flux will radiate widely and will be visible as a broad ‘hard’ pulse. We predict that such flux will appear at phases $\sim 0.35 - 0.5$ after the radio pulse. Ögelman (1994) has noted such a hard ‘magnetospheric’ pulse component in young pulsars and has shown that it connects spectrally onto the high-energy power-law emission. A second X-ray pulse will result from softer flux with a roughly blackbody spectrum emitted from hotter regions near the magnetic axis on the young star’s surface, due both to anisotropic magnetic opacities and to heating by backflowing particles from acceleration zones (Arons 1983). These soft pulses will lie near phase 0, but should again

be quite broad, due to wide emission zones and general relativistic bending of the photons near the neutron star surface. The radio emission at $\sim 10 - 100$ stellar radii should not suffer this effect. Several young pulsars, have in fact been observed to have hard and soft X-ray pulses shifted in phase, in broad agreement with this picture (*eg.* PSR1055-52: Ögelman and Finley 1993; PSR0656+14: Córdoba *et al.* 1991, Finley *et al.* 1992; Geminga: Halpern and Ruderman 1993; and Vela: Ögelman 1994). When α is close to 90° emission may be visible from both caps and from both gaps, complicating the profiles. A third, primarily unpulsed soft X-ray component can be present due to the initial cooling of the hot neutron star; following Ögelman (1994) we expect this to be significant only for young ($10^4\text{y} \leq \tau_c \leq 10^6\text{y}$) neutron stars where the surface T is still large, but the gap luminosity is relatively small.

At present optical pulse profiles are available only for the Crab, Vela and PSR0540-69 pulsars. For the Crab, correspondence of the optical and γ -ray profiles indicates that optical emission is produced over much of the outer gap. However, for the Vela profile the optical pulse is substantially narrower than that of the high energy emission. The phase and width of the pulse are consistent with an origin near the null charge surface (*c.f.* Figure 2). PSR0540-69 has a broad pulse with two peaks (Middleditch and Pennypacker 1985, Gouiffes *et al.* 1992) consistent with a line of sight cutting fairly high on an outer gap. Optical detections have however also been established for Geminga (Halpern and Tytler 1988) and suggested for PSR0656+14 and PSR1509-58 (Caraveo *et al.* 1994a,b). For the former two pulsars the optical emission may be from the Rayleigh-Jeans tail of the thermal flux from the heated polar cap, although non-thermal gap emission is preferred. PSR1509-58, however, if correctly identified at $m_r \sim 21$ must be dominated by non-thermal gap emission. This counterpart is bright enough to allow determination of an accurate pulse profile; in our model we would expect a single broad peak of emission aligned with the hard X-ray pulse (*i.e.* at phase ~ 0.3 with respect to the radio peak).

3. Crab Polarization Results

Interpretation of the Crab pulsed emission has long proved problematic. It is clear from the alignment across a wide spectrum that the radio-optical-X- γ emission from the main pulse and interpulse arises from similar zones, which we identify with the outer magnetosphere gap (although the intensity weighting along the gap surface will differ significantly for the different energy bands). We follow other authors in identifying the precursor with the normal radio pulse. Confusion arises however because the optical pulse exhibits a strong double sweep in the polarization position angle – this has long been interpreted as surface emission in a two-pole RVM fit with $\alpha \approx 90^\circ$ (*e.g.* Narayan and Vivekanand 1982). Since the Crab is the only source for which polarization information is presently available from the high energy region, this association has been very influential in the interpretation of other γ -ray pulsars.

Adopting the same premise as the rotating vector model, (Radhakrishnan and Cooke 1969)

namely that the polarization vector of the emission is set by the local magnetic field, we can similarly compute the position angle swing through the pulse in our outer gap picture. We compute the vector radius of curvature of the field line at the emission point, project this on the plane of the sky, follow aberration variations, and average the position angles from all regions contributing to a given pulse phase to obtain the model polarization sweep. Remarkably, because of the combination of emission from a range of altitudes in the magnetosphere, our model produces an initial sweep from the leading edge of the outer gap (the first pulse), a reversal and a final sweep in the second pulse. This behavior is obtained precisely for the viewing angles that produce the observed $\sim 140^\circ$ profile width. The left panels of figure 5 shows the optical polarization position angle variation (from INT data, Smith, *et al.* 1988) along with a high energy pulse profile from BATSE. Figure 5 also shows model results with the viewing angle chosen only to match the observed pulse width and separation. While it is gratifying that the pulse profile matches well to the data, it is remarkable that the corresponding polarization sweep shows a striking similarity to the observed data, as well. We consider this a major success of our model. With 10m class telescopes and modern detectors it should be possible to obtain polarization data for Vela,

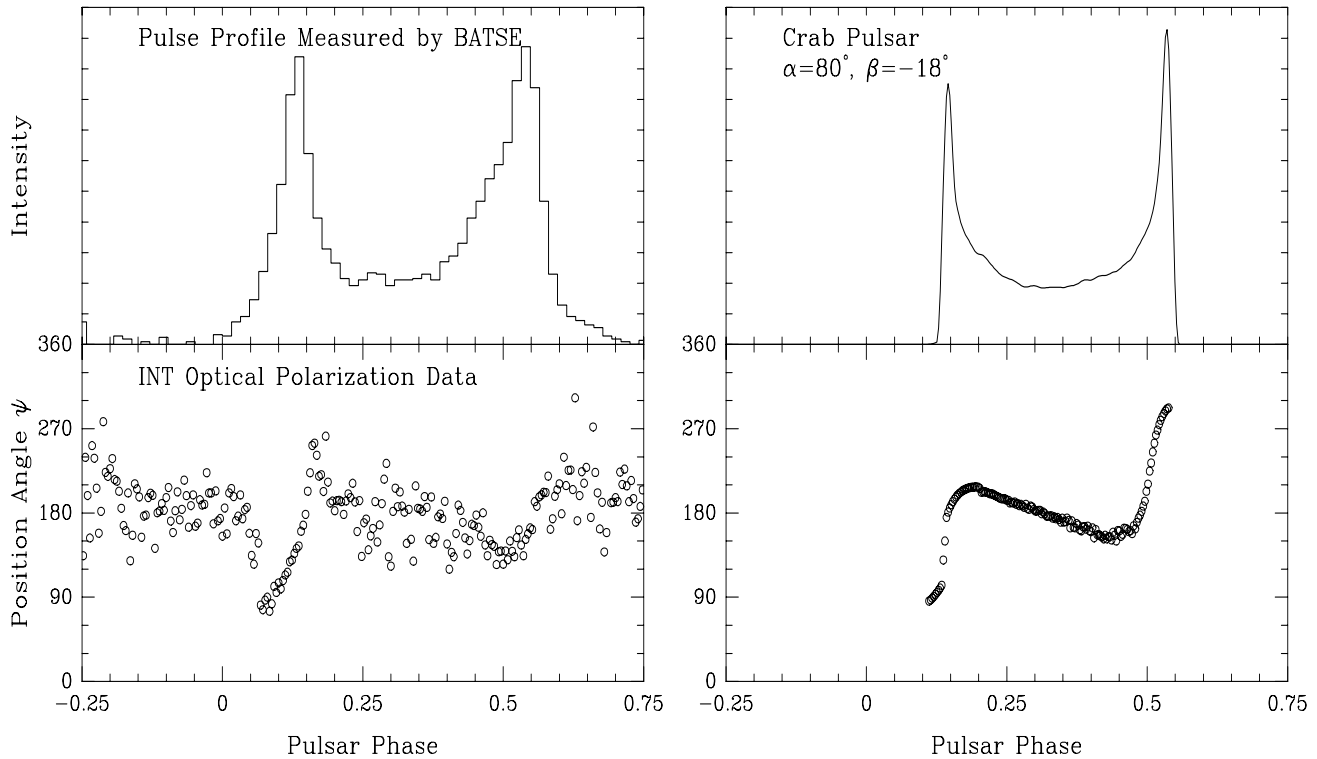


Fig. 5.— Crab pulsar profiles and polarization sweep. Left: light curve data from BATSE (Fishman, GRO Newsl.,1, 6), INT optical polarization data (Smith *et al.* 1988). Right: Model results for Crab outer gap.

PSR1509-58 and PSR0540-69, as well. These would be particularly important in motivating an emission location in the lower portions of the outer gap – since double sweeps generally occur only for $\alpha \gtrsim 70^\circ$, $\zeta \lesssim 70^\circ$, we expect most of these pulsars to show a single sweep of position angle.

4. Population Estimates

In addition to allowing acceptable models for individual pulsars, it is important for a γ -ray emission picture to reproduce the population as a whole. To test our model on this front, we have assumed that magnetic inclinations are random at birth and that the observer orientation is also random and have integrated the beaming fractions and detection probabilities for the radio and γ -ray emission over a population of young ($\tau < 10^{5.5}\text{y}$) pulsars. For the radio emission we have adopted conventional beaming fraction relations ($W = 6.5^\circ P^{-1/3}$ LM; $W = 5.8^\circ P^{-1/2}$ Rankin 1993). The results for the fraction of all young pulsars detectable in the two bands are shown in Figure 6 for the LM beaming law; values for Rankin’s beaming law differ by only a few percent. We have also considered how the results might be affected by alignment torques secularly decreasing α , but with typical alignment timescales $\sim 10^7\text{y}$ (LM) the differences in detection fractions are very small. Uncertainty in the $P - \dot{P}$ dependence of the gap width makes these fractions slightly uncertain; improved estimates of gap closure can remedy this.

Our population estimates show good agreement with present limited data. First, as is well known, the mean radio beaming fraction of these young pulsars, 0.27, leads to a pulsar birthrate reasonably consistent with the galactic supernova rate. Second, roughly 1/3 of the radio selected pulsars should not be visible in γ -rays, to a consistent luminosity threshold. Of the young radio pulsars monitored, several do in fact have upper limits on their efficiency of γ -ray production lower than that of the known emitters (Thompson 1994). Thus with ~ 5 radio pulsars detected in γ -rays it is not surprising that significant upper limits exist for PSR0656+14 and PSR1929+10; non-detection for ~ 2 pulsars should be due to γ beaming. There is also a very strong upper limit for PSR1951+32, but this is probably a mildly recycled pulsar and has a dipole field roughly an order of magnitude lower than the young pulsars. Because of decreased synchrotron emissivity and difficulty in gap closure and inverse Compton scattering photon production, we would not expect this to be an efficient γ -ray pulsar. True millisecond pulsars are similarly poor targets for magnetospheric γ -ray emission.

Finally, because of the large γ -ray beams, the existence of objects such as Geminga not detected in the radio is not surprising. Indeed, scaling from the the 5 radio pulsar detections, we expect ~ 12 non-radio pulsars to be visible in γ -rays to flux levels comparable to the faintest radio selected object, in agreement with the observationally motivated estimates of Helfand (1994). We thus expect most of the ~ 20 unidentified galactic point sources to be young pulsars. In most cases identification of the pulse period will be very difficult: X-ray emission, such as that used to

find the period of Geminga (Halpern and Holt 1992) offers the best hope, but most sources will be 3-10 times more distant, so the count rates will be low. Support for the pulsar hypothesis may be obtained by finding the expected hard Inverse Compton Scattering spectra above 100MeV, or in some cases by association with old supernova remnants.

It is important to note that theories placing the principal γ -ray production in acceleration gaps at the polar cap (Daugherty and Harding 1982, Harding, Ozernoy and Usov 1994; Sturmer and Dermer 1994) have great difficulty in meeting the population test. These models cannot easily produce the range of pulses with bridge emission observed. In particular, to produce wide pulses these models require very small $\alpha \lesssim 10^\circ$ with the observer line of sight ζ nearly aligned with the rotation axis Ω to intercept this small pole (Harding and Daugherty 1993, Dermer and Sturmer 1994). Even *if* pulsars are preferentially born with aligned magnetic axes (a hypothesis not supported by the radio data), the present significant number of detections coupled with the small beaming fraction in these models already implies an enormous birthrate of young pulsars, typically $\gtrsim 30\times$ the galactic supernova rate. We consider this to be unacceptable.

Thus while some γ -rays may be produced in polar gaps, this cannot account for the emission

Detection Probabilities for Young Pulsars

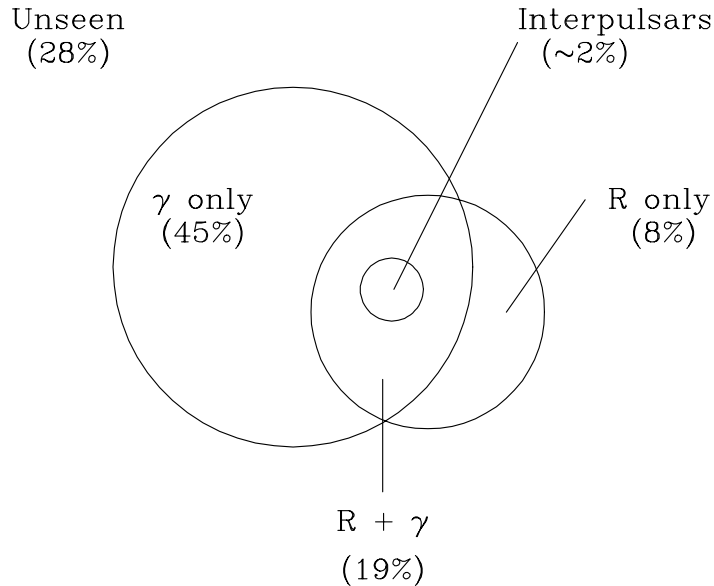


Fig. 6.— Venn diagram for pulsar detectability (beaming fractions). Random magnetic inclinations, high energy emission from both poles and radio beaming factors from LM are assumed. Values are from an integration over pulsars with $\text{Log}(B) = 12.5$ and $\tau_c < 10^{5.5}\text{y}$.

presently observed from radio pulsars. The energetic arguments used in these models to estimate γ fluxes will carry over to the outer gaps in many cases. The processes converting the primary current to the observed γ emission will however be quite different. Accurate models are not yet available for the outer magnetosphere (CR94), so that luminosity laws for γ -ray pulsars must at present remain phenomenological.

5. Conclusions

We have computed the expected pulse shapes and beaming fractions for γ -ray emission from young radio pulsars in a model of charge acceleration in the outer magnetosphere. The results bear a strong resemblance to γ -ray pulse profiles detected by CGRO. In addition our model reproduces the phase relationships between the radio emission and the γ -ray pulse. Observed X-ray and optical pulsations find a natural interpretation in our geometric picture, as well. Important connections between radio pulse and polarization properties resulting from the viewing angle and expected γ -ray profiles have also been established – these give useful predictions for individual pulsars and allow strong tests of the model. We further find that the polarization properties of the Crab pulsar, with emission arising in the upper magnetosphere are easily explained in our model; this supercedes previously confusing interpretations of the polarization data. Finally, the numbers of objects detected in the radio and γ -ray channels are as expected for a population of young pulsars and we infer that most of the unidentified galactic plane sources will be pulsars.

These results are based principally on the *geometry* of the emission region and are thus relatively free from uncertainties in details of the emission process. We are in the process of generating quantitative models for the radiation produced in the upper magnetosphere, but complicated non-linear models will be needed to give accurate results. Previous estimates of outer gap spectra and fluxes (CHR88, Ho 1990) give rough estimates of the total energy available, but do not give accurate results for the observable flux or spectrum. Nonetheless, the dominant physical processes in this outer gap have already been identified by CHR88. The substantial amendments needed for a realistic model, however, mean that spectral results are not yet available.

We feel that the success of our geometrical sums firmly establishes the location of the γ -ray production in the outer magnetosphere and thus resolves the long standing debate with polar cap models in favor of an outer gap picture. Unless similar results can be duplicated by polar models, we feel that these models are not viable and efforts to compute the spectrum and luminosity from the polar cap site cannot explain the bulk of the observed pulsar emission. Much work remains to be done to provide a full picture of the origin of pulsar gamma rays, but assignment of the radiation site gives good hope for further progress. In particular CR94 show that the radiation processes vary strongly with altitude, and that these variations can be mapped directly to pulse phase. Thus phase resolved spectra provide a keen diagnostic for refining global emission models.

Ultimately, detailed comparison with observed profiles should allow us to probe the inertia and current perturbations that are not followed in the present calculation. Understanding of these will help greatly in unraveling the mechanics of the pulsar acceleration process and in producing a self-consistent model of the pulsar magnetosphere. Thus γ -ray measurements can become an important tool in deciphering the puzzle of the pulsar phenomenon.

Support for this work was provided by NASA grants NAGW-2963 and NAG5-2037. We are grateful to Jim Chiang and Joe Fierro for important discussions on the EGRET observations that improved this paper. We also thank F. Graham Smith and Jamie Biggs for sharing the Crab optical data.

Table 1: Young Pulsar Parameters

PSR	$P(\text{ms})$	$\log B(G)$	$\log \tau(y)$	$\log \dot{E}(\text{erg/s})$	L_γ/\dot{E}^a	δ^b	Δ^c	$\alpha(^{\circ})^d$	$\beta(^{\circ})$	X-rays ^e
γ-ray Pulsars										
B0531+21	33	12.6	3.10	38.65	0.004	0.05	0.40	80	-18	h
B1509–58	150	13.2	3.19	37.25	0.012 ^f	0.31	~ 0	60	-15 ^d	h
B0833–45	89	12.5	4.05	36.84	0.012	0.11	0.43	65	+14	s,h
B1706–44	103	12.5	4.24	36.53	0.024	0.21	0.32	42	+25	s?,h
B0630+17	237	12.2	5.53	34.54	$\sim 0.1-0.3$		0.49	25 ^d	+50 ^d	s,h
B1055–52	197	12.0	5.73	34.48	0.2	0.22	0.32	70	-8	s,h
Candidates										
B0540–69	50	12.7	3.22	38.17			$\sim .3^g$			h
B1951+32	40	11.7	5.03	36.57						...
B0656+14	385	12.7	5.05	34.58				8	+8	s?
B0355+54	156	11.9	5.75	34.66				51	+4	...
B1929+10	227	11.7	6.49	33.59				31	+20	s?
B0950+08	253	11.4	7.24	32.75				170	+5	...

^aassumed beaming fraction 0.5

^bradio pulse – first γ ray peak separation (phase units)

^c γ pulse width (phase units)

^destimated from γ -ray data, when available. Values uncertain for Geminga.

^es=soft flux from surface/heated polar cap, h=hard flux from base of outer gap

^f0.1-1 MeV flux only – not detected by EGRET

^gestimated from X-ray, optical, radio data.

REFERENCES

- Arons, J. 1983, ApJ, 266, 215
- Caraveo, P.A., Bignami, G.F. and Mereghetti, S. 1994, ApJ, in press
- Caraveo, P.A., Mereghetti, S. and Bignami, G.F. 1994, ApJ, in press
- Cheng, K.S., Ho, C., and Ruderman, M. A. 1986, ApJ, 300, 522 (CHR)
- Chiang, J. and Romani, R.W. 1992, ApJ, 400, 629
- Chiang, J. and Romani, R.W. 1994, ApJ, submitted (CR94)
- Córdova, F.A. *et al.* in *Extreme Ultraviolet Astronomy*, eds. R.F.Malina and S. Bowyer, (Pergamon Press), 30
- Daugherty, J.K. and Harding, A.K. 1982, ApJ, 252, 337
- Dermer, C.D. and Sturmer, S.J. 1994, ApJ, 420, L75
- Fierro, J.M., *et al.* 1993, ApJ, 413, L27
- Gouiffes, C., Finley, J.P. and Ögelman, H. 1992, ApJ, 394, 581
- Halpern, J.P. and Holt, S.S. 1992, Nature, 357, 222
- Halpern, J.P. and Ruderman, M. 1993, ApJ, 415, 286
- Halpern, J.P. and Tytler, D. 1988, ApJ, 330, 201
- Harding, A.K. and Daugherty, J 1993, in *Isolated Pulsars*, eds K.A. van Riper, R. Epstein, and Ho, C. (New York: Cambridge), 279.
- Harding, A.K., Ozernoy, L.M. and Usov, V.V. 1994, MNRAS, in press.
- Helfand, D.J. 1994, MNRAS, in press.
- Lyne, A.G. and Manchester, R.N. 1988, MNRAS, 234, 477 (LM)
- Mayer-Hasselwander, H.A. *et al.* 1994, ApJ, in press.
- Middleditch, J. and Pennypacker, C. 1985, Nature, 313, 659
- Narayan, R. and Vivekanand, M. 1982, A&A, 113, L3
- Nolan, P.L., *et al.* 1993, ApJ, 409, 697
- Ögelman, H. 1994, in “Lives of Neutron Stars”, eds. J. van Paradijs and A. Alpar (Kluwer), in press
- Ögelman, H., Finley, J. P., 1993, ApJ, 413, L31
- Phillips, J.A. 1990, ApJ, 361, L57
- Radhakrishnan, V. and Cooke, D.J. 1969, Astrophys. Lett., 3, 225
- Rankin, J.M. 1990, ApJ, 352, 247

Rankin, J.M. 1993, ApJ, 405, 285

Smith, F.G., *et al.* 1988, MNRAS, 233, 305

Sturmer, S.J. and Dermer, C.D. 1994, ApJ, 420, L79

Thompson, D.J., *et al.* 1992, Nature, 359, 615

Thompson, D.J. 1994, in preparation

Ulmer, M. P. 1994, IAU Colloquium 142, submitted to ApJS

Ulmer, M. P. *et al.* 1993, ApJ, 417, 738